Kinetic Theory of Laser Filamentation in Plasmas

Eduardo M. Epperlein
Laboratory for Laser Energetics, University of Rochester, 250 East River Road, Rochester, New York 14623-1299
(Received 30 July 1990)

The classical theory of laser thermal filamentation in a homogeneous plasma has been extended to include the effects of nonlocal electron heat transport. The new theory reduces the instability threshold and predicts an optimum perturbation wavelength that maximizes the spatial growth. Theoretical predictions suggest that the thermal mechanism, rather than the ponderomotive one, may explain the experimental observation of filaments by Young *et al.* [Phys. Rev. Lett. **61**, 2336 (1988)]. In general, for conditions typical of inertial-confinement fusion, the thermal filamentation instability is expected to dominate.

PACS numbers: 52.40.Nk, 42.65.Jx, 52.25.Fi, 52.35.Nx

The study of the laser filamentation instability is of particular importance to inertial-confinement fusion (ICF). The filamentation instability results from spatial modulations in the incident laser intensity profile that give rise to changes in the plasma refractive index, which, in turn, can amplify the initial level of modulation. Resultant high-intensity filaments can then aggravate other deleterious laser-plasma instabilities.[1]

The filamentation can be identified as either ponderomotive[2] or thermal,[3] depending on whether the changes in refractive index are caused directly by the laser ponderomotive force or indirectly by inverse-bremsstrahlung heating, respectively. In this Letter, the linear theory for thermal filamentation is extended to include the effects due to nonlocal electron heat transport. The improved transport treatment predicts heat-flux inhibition at short perturbation wavelengths, which then allows for higher temperature, density, and refractive-index modulations. The resulting theory substantially modifies the classical results by reducing the instability threshold and giving rise to an optimum perturbation wavelength that maximizes the spatial growth. In contrast, theories based on classical heat flow yield constant growth rates over a wide range of wavelengths.[3] Theoretical predictions also suggest that the thermal mechanism should dominate over the ponderomotive one for most cases of interest to ICF. Specifically, the new kinetic theory provides an alternative explanation for experimental observations of filaments such as those recently reported by Young *et al.*[4]

The stability analysis follows essentially the approach adopted in previous articles.[2,3] We consider the growth of a plane electromagnetic wave of amplitude E,

$$\hat{\mathbf{x}}E\cos(k_0z-\omega t),$$

subject to a small perturbation e with y dependence of the form

$$\hat{\mathbf{x}}[e_1\cos(k_0z-\omega t)+e_2\sin(k_0z-\omega t)]\exp(Kz-iky),$$

where k is the perturbation wave number and K is the spatial growth rate. (The directions between the perturbation wave vector and the electric-field polarization are chosen so as to maximize K.[2]) Substituting this form of electric field into the electromagnetic wave equation in a plasma, and using the slowly-varying-envelope approximation, we obtain (assuming $K\ll k\ll k_0$)

$$2k_0Ke_1+k^2e_2=0, \tag{1a}$$

$$-2k_0Ke_2+k^2e_1+\frac{\omega^2}{c^2}\frac{n}{n_c}E\frac{n_1}{n}=0, \tag{1b}$$

where n/n_c is the ratio of background to critical density and n_1 is the perturbed density. These equations are then coupled to the linearized momentum and energy balance equations, respectively,

$$\frac{n_1}{n}=-\frac{T_1}{T}-\left(\frac{Z}{Z+1}\right)\frac{e_1}{E}\frac{v_{\rm osc}^2}{2v_t^2}, \tag{2}$$

$$\frac{T_1}{T}=\frac{2S}{\kappa Tk^2}\frac{e_1}{E}, \tag{3}$$

where S is the background inverse-bremsstrahlung heating rate, κ is the thermal conductivity, T_1 is the perturbed temperature (assumed equal for electrons and ions), and $v_{\rm osc}/v_t$ (which is the term responsible for the ponderomotive filamentation) is the ratio of the electron oscillatory velocity in the electric field E to its thermal velocity.

Before solving Eqs. (1)–(3) it is important to consider the validity of the heat flow model in Eq. (3). Classically, κ would be the Spitzer-Härm (SH) conductivity $\kappa_{\rm SH}$.[5] However, it has been shown that under conditions where the temperature scale length is shorter than some appropriate electron mean free path λ_e (to be defined later), the SH formula breaks down.[6] Under such circumstances, it is more appropriate to model the energy balance using the electron Fokker-Planck (FP) equation.[6-9] However, instead of solving the FP equation for every stability analysis, it is much more convenient (and less costly in terms of computer time) to appropriately modify κ so as to account for kinetic transport effects.

In order to accomplish this, the FP code[7,8] SPARK has been adapted to calculate T_1/T for a given e_1/E, in an initially homogeneous plasma. The effective conductivity is then calculated by defining

$$\kappa = \frac{2S}{k^2 T}\frac{e_1/E}{T_1/T}.$$

The code is run with a sinusoidal spatial modulation (of arbitrary amplitude) in the laser field until a steady temperature modulation is achieved. As expected, in the limit of large wavelengths (or small k), $\kappa \rightarrow \kappa_{SH}$. In the small-wavelength limit, however, it is found that $\kappa < \kappa_{SH}$. Such a phenomenon, which is commonly known as flux inhibition,[6] occurs as a result of nonlocal transport of heat-carrying electrons (with kinetic energies of about 7 T) across several wavelengths. Since these high-energy electrons cannot equilibrate instantaneously with the thermal electrons (by virtue of their relatively low collisionality) they are able to establish a smoother density gradient in phase space than the thermal component, and hence, reduce the effectiveness of the heat flow. This type of effect, first identified by Bell[10] in the context of ion waves, has also been demonstrated in two-dimensional thermal transport simulations using SPARK.[7,9]

The spectrum of κ/κ_{SH} as a function of $k\lambda_e$ has been obtained and plotted in Fig. 1. Here, κ has been appropriately normalized by defining $\lambda_e = T^2/4\pi ne^4 \times (Z+1)^{1/2}\ln\Lambda$ as the effective delocalization length (or stopping length) of an electron. Such a definition accounts for the balance between electron spatial diffusion and thermalization.[11] A very accurate fit to the data points in Fig. 1 is obtained by using $\kappa/\kappa_{SH} = [1+(30k\lambda_e)^{4/3}]^{-1}$ (see solid curve). In contrast, a Fourier analysis of the heat-flow formula proposed by Luciani, Mora, and Virmont[12] would yield $\kappa/\kappa_{SH} = [1+(30k\lambda_e)^2]^{-1}$, which has an incorrect asymptotic dependence for large $k\lambda_e$ (see also Ref. 9).

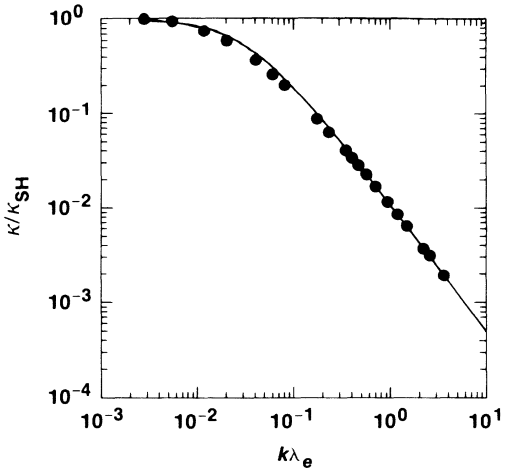

FIG. 1. Ratio of effective conductivity κ to Spitzer-Härm conductivity κ_{SH} as a function of $k\lambda_e$, where k is the perturbation wave number and λ_e is the electron delocalization length. Solid circles correspond to SPARK data, and the solid curve is a numerical fit to that data.

It must be emphasized that the heat-flow reduction depicted in Fig. 1 cannot be adequately modeled by the usual flux-limiter method,[13] where the magnitude of the classical heat flow $\mathbf{q} = -\kappa_{SH}\nabla T$ is limited to some arbitrary fraction f of the free-streaming heat flow $q_f = nmv_t^3$ through the formula $\kappa/\kappa_{SH} = [1+|\mathbf{q}/fq_f|]^{-1}$. This is due to the fact that the flux limiter depends on the *local* temperature scale length $T/|\nabla T|$, whereas the actual heat-flow reduction should depend on the *global* temperature scale length k^{-1}. Moreover, since the temperature perturbation in the stability analysis is assumed to be infinitesimal, $|\mathbf{q}/fq_f| \ll 1$, which makes the flux limiter virtually inactive.

The growth rate based on Eqs. (1)–(3) and the modified κ is given by

$$K = \frac{k}{2\sqrt{\varepsilon}}\left[2\frac{n}{n_c}\left(\gamma_p + \gamma_T[1+(30k\lambda_e)^{4/3}]\frac{\omega^2}{k^2c^2}\right) - \frac{k^2c^2}{\omega^2}\right]^{1/2},$$

where $\varepsilon = 1 - n/n_c$, and (using the notation adopted in Ref. 14)

$$\gamma_p = \frac{1}{4}\left(\frac{Z}{Z+1}\right)\frac{v_{osc}^2}{v_t^2},$$

$$\gamma_T = c^2 S/\omega^2 \kappa_{SH} T.$$

In the limit as $30k\lambda_e \ll 1$ and $\gamma_p = 0$ (i.e., no ponderomotive effect) we recover the classical dispersion relation for thermal filamentation,[3,14] which yields a maximum growth rate in the limit as $k \rightarrow 0$, i.e.,

$$(K_{max})_T^{SH} = \frac{\omega}{c}\left(\frac{1}{2\varepsilon}\frac{n}{n_c}\gamma_T\right)^{1/2}.$$

In the kinetic limit ($30k\lambda_e \gg 1$), an optimum value of $k = (k_{max})_T^{FP}$ can be derived which maximizes K, i.e.,

$$(k_{max})_T^{FP} = \frac{\omega}{c}\left[\frac{2}{3}\frac{n}{n_c}\gamma_T\left(30\lambda_e\frac{\omega}{c}\right)^{4/3}\right]^{3/8} \quad (4)$$

and

$$(K_{max})_T^{FP} = \frac{\omega}{c\sqrt{2\varepsilon}}\left[30\lambda_e\frac{\omega}{c}\left(\frac{2}{3}\frac{n}{n_c}\gamma_T\right)^{3/4}\right]. \quad (5)$$

The optimum growth rate for ponderomotive filamentation can be obtained by setting $\gamma_T = 0$ (thus making it insensitive to nonlocal transport effects), and is found to be[2,14]

$$(K_{max})_p = \frac{1}{2}\frac{\omega}{c}\frac{n}{n_c}\frac{\gamma_p}{\sqrt{\varepsilon}}, \quad (6)$$

with

$$(k_{\max})_p = \frac{\omega}{c}\left(\frac{n}{n_c}\gamma_p\right)^{1/2}. \quad (7)$$

To illustrate the results presented so far, let us consider the recent experiment by Young *et al.*,[4] designed to demonstrate the occurrence of laser filamentation. Using their experimental conditions (i.e., $I=4.2\times10^{13}$ W/cm^2, $T=0.8$ keV, $n/n_c=0.1$, $\lambda_{\text{laser}}=1.06$ μm, $Z=3.5$, and $k=k_{\text{expt}}=1500$ cm^{-1}) K is plotted as a function of k in Fig. 2. Here, the improved theory for thermal filamentation (curve a) clearly enhances the growth rate well above the classical value (curve b), and gives rise to a well-defined optimum K (as opposed to fairly constant growth as $k\to 0$). This is not surprising since the experimental conditions correspond to the kinetic limit of the instability, i.e., $k_{\text{expt}}\lambda_e \approx 2.7$ and $\kappa/\kappa_{\text{SH}} \approx 2.8\times10^{-3}$. One should also note by comparing with the ponderomotive filamentation result (curve c) that $(K_{\max})_T^{\text{FP}}/(K_{\max})_p \sim 3$ and $k_{\text{expt}} \sim (k_{\max})_T^{\text{FP}} \sim (k_{\max})_p$. Thus, the conclusion reached by Young *et al.*,[4] that their experiment gave direct evidence of ponderomotive filamentation needs to be revised. Their conclusion was in part based on a threshold condition, arbitrarily defined as one e-fold increase in laser intensity modulation, which for a plasma of length L implies $2KL=1$.[1] Such a criterion, however, fails to account for the light intensity that is required to produce the level of density modulation $\delta n/n$ needed for experimental observation. Indeed, a simple estimate of density modulation using pressure balance (neglecting thermal effects), i.e., $\delta n/n = 1-\exp(-\gamma_p)$,[2] predicts intensities of $\sim 10^{15}$ W/cm^2 in order to yield the 10% modulation observed in Ref. 4. Since $L=300$ μm, this implies at least a factor of 10 (or greater than two e-fold) increase in laser intensity. Therefore, based on linear growth rates, the new kinetic theory suggests that the thermal filamentation mechanism may be the more likely candidate to explain the results. For a more definitive conclusion, however, the self-consistent time evolution and nonlinear saturation of the filaments would have to be taken into account.

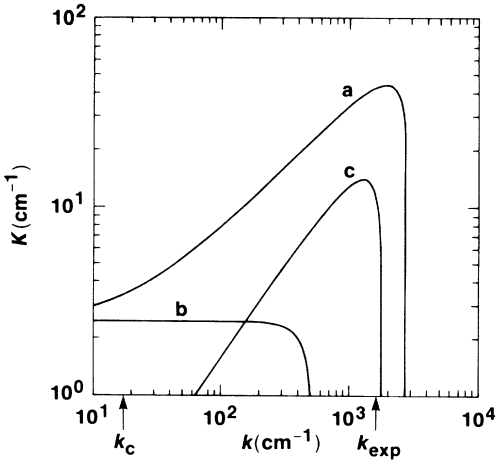

FIG. 2. Plots of spatial growth K (cm^{-1}) as a function of perturbation wave number k (cm^{-1}), for, curve a, thermal (kinetic theory); curve b, thermal (classical theory); and curve c, ponderomotive instability.

In general, comparisons between $(K_{\max})_T^{\text{FP}}$ and $(K_{\max})_p$ may be obtained by expanding Eqs. (5) and (6),

$$(K_{\max})_T^{\text{FP}} = 1.98\times10^{-2}\frac{(\ln\Lambda)^{1/2}ZI^{3/4}}{\varepsilon^{7/8}T^{7/4}\phi^{3/4}(1+1/Z)^{1/2}}\left(\frac{n}{n_c}\right)^{5/4}\mu\text{m}^{-1},$$

$$(K_{\max})_p = 2.93\times10^{-2}\frac{\lambda_{\text{laser}}I}{\varepsilon T(1+1/Z)}\left(\frac{n}{n_c}\right)\mu\text{m}^{-1},$$

where $\phi=(Z+0.24)/(1+0.24Z)$; I is in units of 10^{14} W/cm^2, T in keV, and λ in μm. Using Eqs. (4) and (7), the respective optimum perturbation wavelengths ($\lambda_{\max}=2\pi/k_{\max}$) are found to be

$$(\lambda_{\max})_T^{\text{FP}} = 15.0\frac{\varepsilon^{3/16}T^{7/8}(1+1/Z)^{1/4}\lambda_{\text{laser}}^{1/2}\phi^{3/8}}{(\ln\Lambda)^{1/4}Z^{1/2}I^{3/8}}\left(\frac{n_c}{n}\right)^{5/8}\mu\text{m},$$

$$(\lambda_{\max})_p = 10.4\frac{\varepsilon^{1/4}T^{1/2}(1+1/Z)^{1/2}}{I^{1/2}}\left(\frac{n_c}{n}\right)^{1/2}\mu\text{m}.$$

For conditions typical of current direct-drive spherical implosion experiments, i.e., $I=10^{14}$ W/cm^2 (single beam intensity), $T=1$ keV, $n/n_c=0.1$, and $\lambda_{\text{laser}}=0.35$ μm, the predicted growth rates and optimum wavelengths have been calculated for $Z=3.5$ and 35. These are displayed in Table I, together with the laser attenuation rate K_{ib},[15] which has been neglected in the present stability analysis. Since $K_{\max}\gg K_{ib}$, this last assumption is probably justified. Also, the original assumption that $K\ll k\ll_0$ is well satisfied for the conditions considered here.

A criterion for kinetic effects to dominate is that $k > k_c = (30\lambda_e)^{-1}$ (see Fig. 2), or in terms of wave-

TABLE I. Instability growth rates, laser attenuation rates, and optimum wavelengths, for $Z=3.5$ and 35.

	$Z=3.5$	$Z=35$
$(K_{max})_T^{SH}$ (μm^{-1})	5.67×10^{-4}	4.18×10^{-3}
$(K_{max})_T^{FP}$ (μm^{-1})	5.26×10^{-3}	3.71×10^{-2}
$(K_{max})_p$ (μm^{-1})	8.86×10^{-4}	1.11×10^{-3}
$(K_{max})_T^{FP}/(K_{max})_p$	5.93	33.5
K_{ib} (μm^{-1})	5.3×10^{-4}	5.3×10^{-3}
$(\lambda_{max})_T^{FP}$ (μm)	17.6	6.65
$(\lambda_{max})_p$ (μm)	36.1	32.6

length,

$$\lambda<\lambda_c=60\pi\lambda_e$$

$$=6.58\times10^3\frac{T^2\lambda_{laser}^2}{\ln\Lambda(Z+1)^{1/2}}\left[\frac{n_c}{n}\right]\mu m\,.$$

Once again, for the same typical ICF conditions, $\lambda_c\sim676$ μm (for $Z=3.5$) and $\lambda_c\sim239$ μm (for $Z=35$), so that one would expect the kinetic regime to prevail over a wide range of wavelengths. With this being the case, one would also expect that $(\lambda_{max})_T^{FP}<(\lambda_{max})_p$, and not the other way around as has been previously predicted.[1,14]

In conclusion, a new theory of laser filamentation has been derived that takes into account nonlocal electron transport. The predicted reduction in the electron thermal conductivity at short perturbation wavelengths allows for enhanced temperature and density modulations, which in turn enhance the growth rate of the laser thermal filamentation. For typical ICF conditions, the theory also suggests that the thermal mechanism would dominate over the ponderomotive one. This has been illustrated by correlating the growth-rate predictions with a recent experiment.

This work was supported by the U.S. Department of Energy Division of Inertial Fusion under Agreement No. DE-FC03-85DP40200 and by the Laser Fusion Feasibility Project at the Laboratory for Laser Energetics which has the following sponsors: Empire State Electric Energy Research Corporation, New York State Energy Research and Development Authority, Ontario Hydro, and the University of Rochester.

[1]W. L. Kruer, Comments Plasma Phys. Controlled Fusion **9**, 63 (1985).

[2]P. Kaw, G. Schmidt, and T. Wilcox, Phys. Fluids **16**, 1522 (1973).

[3]M. S. Sodha, A. K. Ghatak, and V. K. Tripathi, in *Progress in Optics,* edited by E. Wolf (North-Holland, Amsterdam, 1976), Vol. 13, p. 169.

[4]P. E. Young, H. A. Baldis, R. P. Drake, E. M. Campbell, and K. G. Estabrook, Phys. Rev. Lett. **61**, 2336 (1988); P. E. Young, Comments Plasma Phys. Controlled Fusion **12**, 53 (1988).

[5]L. Spitzer, Jr., and R. Härm, Phys. Rev. **89**, 977 (1953).

[6]D. R. Gray and J. D. Kilkenny, Plasma Phys. **22**, 81 (1980); A. R. Bell, R. G. Evans, and D. J. Nicholas, Phys. Rev. Lett. **46**, 243 (1981).

[7]E. M. Epperlein, G. J. Rickard, and A. R. Bell, Phys. Rev. Lett. **61**, 2453 (1988).

[8]E. M. Epperlein, G. J. Rickard, and A. R. Bell, Comput. Phys. Commun. **52**, 7 (1988).

[9]E. M. Epperlein, in Proceedings of the Topical Conference on Research Trends in Nonlinear and Relativistic Effects in Plasmas, San Diego, California, February 1990 (to be published).

[10]A. R. Bell, Phys. Fluids **26**, 279 (1983).

[11]J. R. Albritton, E. A. Williams, I. B. Bernstein, and K. P. Swartz, Phys. Rev. Lett. **57**, 1887 (1986).

[12]J. F. Luciani, P. Mora, and J. Virmont, Phys. Rev. Lett. **51**, 1664 (1983).

[13]R. C. Malone, R. L. McCrory, and R. L. Morse, Phys. Rev. Lett. **34**, 721 (1975).

[14]A. J. Schmitt, Phys. Fluids **31**, 3079 (1988).

[15]T. W. Johnston and J. M. Dawson, Phys. Fluids **16**, 722 (1973).